INSTITUTE OF PHYSICS PUBLISHING NANOTECHNOLOGY
Nanotechnology **15** (2004) S270–S275 PII: S0957-4484(04)70066-5

Near-field optical microscopy of polymer-based films with dispersed terthiophene chromophores for polarizer applications

A Ambrosio[1,4], M Alderighi[1], M Labardi[1], L Pardi[1], F Fuso[1], M Allegrini[1], S Nannizzi[2], A Pucci[3] and G Ruggeri[3]

[1] INFM, Dipartimento di Fisica 'E Fermi', Università di Pisa, Via F. Buonarroti 2, I-56127 Pisa, Italy
[2] Dipartimento di Chimica e Chimica Industriale, Università di Pisa, Via Risorgimento 35, I-56126 Pisa, Italy
[3] INSTM, Dipartimento di Chimica e Chimica Industriale, Università di Pisa, Via Risorgimento 35, I-56126 Pisa, Italy

E-mail: ambrosio@df.unipi.it

Received 8 October 2003, in final form 9 February 2004
Published 2 March 2004
Online at stacks.iop.org/Nano/15/S270 (DOI: 10.1088/0957-4484/15/4/029)

Abstract
Linear dichroic properties of polyethylene films containing a dispersion of terthiophene-based chromophore molecules are investigated by using a scanning near-field optical microscope (SNOM). The polarization-modulation technique implemented in our SNOM provides quantitative information on the dichroic ratio of the samples with sub-wavelength space resolution. Optically active domains are identified and their morphology is analysed as a function of the film fabrication parameters, e.g., the drawing ratio and the kind of dispersed chromophore mixture. These investigations complement conventional polarimetry analysis by adding nanometre-scale information on the spatial distribution of the chromophore molecules and their mutual alignment with the host polymer chains.

1. Introduction

Since the first introduction of scanning near-field optical microscopy (SNOM) [1], a great deal of effort has been devoted to broaden the spectrum of optical properties that can be analysed with the sub-wavelength space resolution typical of this technique. Indeed, the non-propagating character of the near-field [2] makes SNOM a unique tool for the assessment of sample performance in the sub-micrometre range, while offering valuable information for a deep understanding of the optical properties at the local scale.

In particular, by combining SNOM with techniques aimed at controlling the polarization state of the light coupled to the near-field probe, optical activity can be successfully investigated. We have exploited polarization-modulation [3] aperture-SNOM (PM-SNOM) to investigate polymer-based films designed as linear polarizers for demanding applications including, e.g., fabrication of liquid crystal displays (LCDs). Generally, highly conjugated terthiophene based chromophores functionalized with alkyl linear lateral chains and different electron-withdrawing groups can be dispersed in the amorphous phase and at the interface between the amorphous and the crystalline phase of ethylene polymers (PE) and oriented by elongation stretching along the drawing (macromolecular) direction according to the pseudo-affine deformation scheme [4]. The stretched films have an excellent dichroic behaviour in the absorption and fluorescence region of the chromophore molecule, suggesting potential applications of these systems as linear polarizers [4]. Our samples consist of a host–guest system, with a small amount of terthiophene-derived dye molecules dispersed in an ultra-

[4] Author to whom any correspondence should be addressed.

high molecular weight polyethylene (UHMW-PE) matrix [4]. Films are obtained by a solution-casting process followed by mechanical drawing. Linear dichroism arises because of the mutual alignment of the chromophore molecules, which exhibit a strong anisotropic absorption due to a linear rod-like conjugated core with the polymer chains organized along the drawing axis [5].

Some polymeric gel processed host–guest polarizers do not follow the pseudo-affine deformation scheme. This observation is attributed to phase separation phenomena between the absorbing guest molecules and the polymer matrix resulting in an immobilization of the dispersed dye during tensile deformation [6–8]. As a consequence, several attempts have been recently performed in order to control and minimize the chromophore aggregation into the polyethylene matrix [6–8]. Several issues are still open to further improve the quality of such polarizing devices. For instance, the homogeneity of the chromophore dispersion is important when device miniaturization is a concern, as in LCDs. Indeed, extended conjugation and high dipole moment enhance aggregation and phase separation phenomena, imposing the use of a relatively small guest concentration. As a consequence, the efficiency of the molecule alignment has to be carefully investigated and correlated with the fabrication parameters, like the drawing ratio and the kind of molecular mixture. Conventional polarimetry, due to its diffraction-limited space resolution [9], cannot be used to gain insight into the sample features at the local scale [10]. On the other hand, approaches based on scanning electron microscopy (SEM), while offering suitable space resolution, provide no direct information on the optical behaviour of the samples.

SNOM-based techniques appear of particular relevance within this context, provided they can be used to reliably compare properties of films produced with different parameters. Such a challenging task can hardly be accomplished through qualitative analysis of the optical properties, that is a rather common approach in near-field microscopy, where local variations of the relevant quantities are typically imaged. As a matter of fact, implementation of PM in a SNOM apparatus [11] opens the way to rich and detailed studies of optical activity at the local scale [12, 13], but at the same time requires special care in data interpretation in order to obtain quantitative results. First of all, the optical activity of the near-field probe, typically a tapered optical fibre in aperture-SNOM, must be duly taken into account in order to prevent masking of the genuine sample properties [14]. We have already demonstrated [15] the feasibility of PM-SNOM measurements with our microscope, using suitable tapered fibres as a probe. Here, we apply this method to investigate stretched polymer films and, following a simple data analysis model [16], we evaluate the dichroic ratio of our samples on the local scale. Although more sophisticated and powerful approaches, based on the Fourier-transform analysis, have recently been proposed [12, 17], our results enable a reliable comparison of samples produced in different experimental conditions, nicely complementing conventional polarimetry analysis aimed at identifying the optimal fabrication conditions.

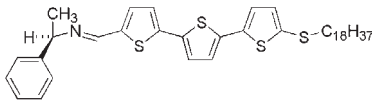

(1*R*-phenylethyl)-5”-thiooctadecyl-[2,2':5',2”]terthien-5-ylmethylidene amine

Figure 1. Chemical structure of our chromophore molecule (right-handed enantiomer).

2. Experimental details

Samples are produced starting from a p-xylene solution of a terthiophene derivative chromophore (3 wt%) and UHMW-PE. The chromophore molecules, whose structure is sketched in figure 1, was synthesized starting from materials previously prepared [4] and using standard methods [18]. Light absorption is in the visible, with a peak around 400 nm, and the molecule exhibits fluorescence emission with a broad spectrum centred at 500–530 nm. The right-handed enantiomer of the terthiophene chromophore and its 50:50 right-handed and left-handed mixture (racemic mixture) are prepared [19]. Samples containing either the racemic mixture or only the right-handed enantiomer are analysed in order to ascertain the possible influence on the linear dichroism of the films [20]. A casting process with solvent evaporation is used to obtain as-cast samples with typical thickness around 100 μm, followed by mechanical drawing accomplished by hand stretching the as-cast sample over a hot plate at $T = 130\,^{\circ}\mathrm{C}$. The stretching process is carried out in order to favour the alignment of polymer chains along the drawing axis. The dispersed chromophore molecules are expected to align along the same direction [21], with a larger concentration close to the upper surface of the cast, as confirmed by SEM microanalysis measurements of the sample cross-section [4].

The PM-SNOM set-up used for the present investigations is an implementation of the home made set-up described in [15]. Polarization control is achieved by sending the laser beam, in this work the Ar^+ line at 488 nm, through a chain consisting of a linear polarizer, an electro-optic modulator (EOM, from Quantum Technology) and a quarter-waveplate. The Ar^+ laser is positioned on a different optical table to avoid vibrations due to the laser fans and the laser beam is sent into the polarization control chain through a single-mode optical fibre, as shown in figure 2(a). To reduce undesired intensity modulation associated with spurious effects in the fibre, an electronic feedback circuit is used to stabilize the laser power within the bandwidth of interest. The main components of this feedback chain (figure 2(a)) are a photodiode collecting a portion of the laser beam and an acousto-optic modulator (AOM) distributing laser power between first and zero diffraction orders. We have checked that, by properly aligning and tuning our set-up, residual intensity fluctuations are below 5%.

The first element of the polarization chain is a linear polarizer that provides a linear polarization at 45° with respect to the EOM axis. The EOM behaves like a controllable waveplate, providing an electrically variable phase delay between the two polarization components of the incoming beam. We obtain a phase delay varying from 0 to 2π by biasing the EOM crystal with a periodic saw-tooth voltage (typical frequency 3–5 kHz). In these conditions, the laser

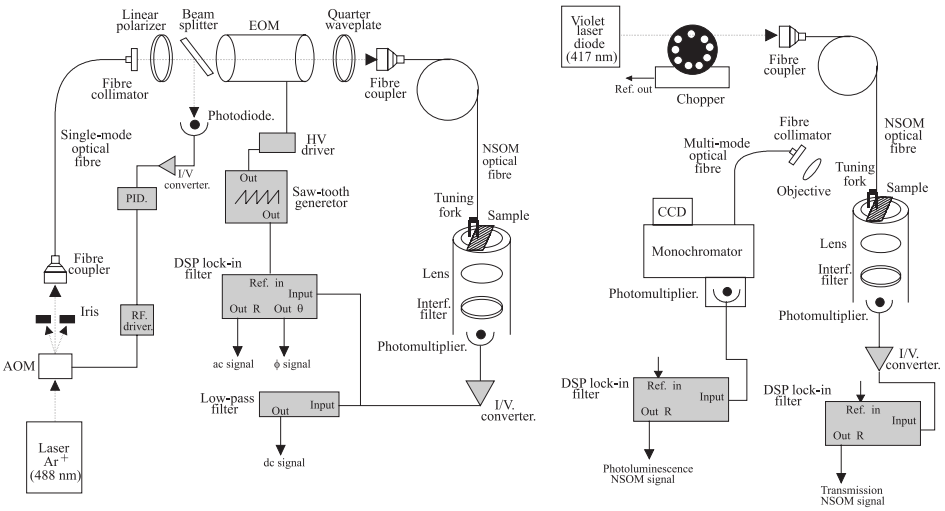

Figure 2. Left: set-up for the PM-SNOM. Right: set-up for near-field photoluminescence spectroscopy.

beam emerging from EOM exhibits time-depending elliptical polarization. Further passage through the quarter-waveplate produces a linear polarization rotating with the same frequency as the bias modulation. In other words, a full, true and continuous control of the polarization direction for the laser light is achieved before launching it into the SNOM fibre probe.

This probe is a commercial (Nanonics Ltd) tapered fibre with a metallized tip (throughput $\sim 10^{-5}$). At the fibre end there is a small aperture (about 100 nm in diameter) which acts as a near-field quasi point-like emitter. We have previously tested the conservation of the injected light polarization direction in the near-field produced by our SNOM fibre by scanning on reference sample surfaces as illustrated in our previous work [15].

We can collect both transmitted and reflected light scattered by the sample surface. Transmitted light is collected by a high numerical aperture (NA) lens and sent to a miniaturized photomultiplier tube (PMT, Hamamatsu R5600U). An output signal from the PMT is sent to both a dual phase lock-in (Stanford SR830) and a low pass electronic filter (Stanford SR650).

PM-SNOM analysis in the transmission configuration is carried out to investigate the anisotropic absorption of the samples at 488 nm as in [22]. In addition, photoluminescence (PL) studies are also carried out as in [23]. A sketch is shown in figure 2(b). For a PL near-field investigation, we use a 417 nm laser diode, close to the absorption peak of chromophore molecules. With this source, intensity modulation is provided by a mechanical chopper before the SNOM optical fibre. PL maps are then acquired at a fixed polarization direction of the exciting light. Emission from the sample is collected in reflection. Through a 0.42 NA, long working distance objective mounted at 45° off the sample surface and an optical fibre, reflected light is sent into a monochromator (Jobin-Yvon Triax320), equipped with a 1200 grooves mm^{-1} grating and a cooled PMT or back illuminated CCD for detection. The transmitted SNOM signal is also simultaneously acquired in order to obtain SNOM transmission images useful for a reference.

A sample area of the order of a few $\mu\mathrm{m}^2$ is typically analysed during a scan and, as customarily accomplished in SNOM, a topography map of the same region is recorded through the shear force method [24] in order to correlate the morphology of the optically active domains with the sample topography.

3. Data analysis

We record the demodulated amplitude (ac) and phase (ϕ) signals from the lock-in, synchronous with the polarization modulation frequency, during the SNOM scans. As already mentioned, we also use a low-pass electronic filter with a cutoff frequency smaller than the PM frequency, in order to acquire a signal (dc) representative of the transmitted intensity averaged over all different polarization states. Quantitative information on the local optical anisotropy of our samples is derived from the optical signals. Following methods available in the literature [16, 25], we produce maps of the local dichroic ratio $\gamma = (I_\parallel - I_\perp)/(I_\parallel + I_\perp)$, $I_\parallel$ and $I_\perp$ being the intensity transmitted by the sample for light polarized along two mutually orthogonal axes that maximize the observed anisotropy. Furthermore, a map of the angle θ between such axes and the polarization direction of the laser light can be useful to better characterize the anisotropic absorption of the film. By using a matrix representation of the polarization state of the radiation, γ and θ local values can be derived from the acquired signals [16]:

$$\gamma = \sqrt{\left[\left(\frac{\mathrm{ac}}{\mathrm{dc}}\right)\cos 2\phi - \left(\frac{\mathrm{ac}}{\mathrm{dc}}\right)_{\mathrm{fibre}}\right]^2 + \left[\left(\frac{\mathrm{ac}}{\mathrm{dc}}\right)\sin 2\phi\right]^2} \quad (1)$$

$$\theta = \frac{1}{2}\arctan\left[\frac{(\frac{\mathrm{ac}}{\mathrm{dc}})}{(\frac{\mathrm{ac}}{\mathrm{dc}})\cos 2\phi - (\frac{\mathrm{ac}}{\mathrm{dc}})_{\mathrm{fibre}}}\right]. \quad (2)$$

These equations account for the residual linear optical activity of the SNOM probe (terms with the subscript 'fibre'). In fact the main point in data processing is that the residual optical activity of the SNOM fibre must be carefully taken into account in order to obtain reliable results [12, 16]. In our set-up, the anisotropy due to the optical fibre is roughly compensated by mechanically stretching the fibre, tightly bent around one fixed point. The maps of the relevant quantities

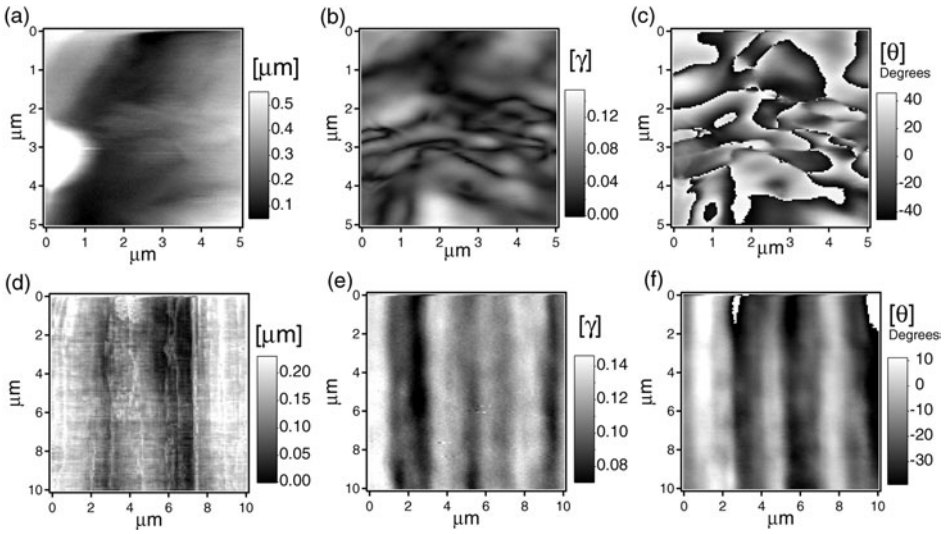

Figure 3. Top: topography (a), γ (b) and θ (c) maps of an as-cast sample. Bottom: ((d)–(f)) corresponding maps of a 30× stretched film. Both samples contain a 50:50 enantiomer mixture. Note that regions with different sizes are imaged for the two samples.

acquired on reference samples (non-dichroic) are practically flat, as expected due to their homogeneity and to the absence of dichroism, and the $(\mathrm{ac}/\mathrm{dc})_{\mathrm{fibre}}$ value can be derived by space averaging over all the scanned area of such reference samples. We have checked the repeatability of the results after several scans, and have found that the residual dichroic ratio of the used probes is smaller than that of the samples under investigation (around 10–20% of the sample dichroic ratio).

4. Results and discussion

Optical activity in our films is expected to be strictly related to the mutual alignment of the anisotropic dye molecules with the polymer chains of the matrix, following the mechanical drawing process. Such an effect is the basis of the macroscopic applications of the films as linear polarizers. Verification of the effect at the mesoscopic range, accessible thanks to the SNOM space resolution, is the first goal of our investigation. According to the results of macroscopic studies on this class of sample [4], the prominent phenomena are due to the linear dichroism of the chromophore molecules, stemming from their mutual alignment with the host polymer chains. Furthermore, the possible effects related to circular dichroism turned out practically negligible in the macroscopic investigations. Nevertheless it has been shown [13, 17] that the effects of birefringence and linear dichroism can be efficiently distinguished in near-field analyses. In our set-up we do not make use of any polarization analyser in front of the detector collecting the transmitted light, so that we are sensitive only to linear dichroism. Our data analysis, based on [16], is indeed aimed at deriving the linear dichroic ratio at the local (mesoscopic) scale. We are planning further implementation of the experimental set-up and of the data interpretation method in order to assess the role of other effects.

We have compared the maps of the optical properties, acquired in transmission, constructed as specified above, for as-cast samples and for films obtained by drawing. An example of our measurements is shown in figure 3, where the top and bottom panels refer to an as-cast and a stretched film (mechanical drawing ratio of 30×), respectively. Striking differences appear, both in the topography and in optical maps (figure 3). In particular, topographical structures elongated along the vertical direction, corresponding to the drawing axis, can be easily seen in the stretched film (figure 3(d)), whereas no elongated morphology appears in the as-cast sample (figure 3(a)). The sample topography is obviously affected by the drawing procedure and the associated formation of the host polymer chains aligned along the drawing axis. This is reflected in a clearly observable change of the morphology between as-cast and drawn samples (figures 3(a) and (d), respectively). We note also, that the average roughness of the as-cast sample is much larger than for the mechanically drawn one, as suggested by the height scale shown close to each map, in spite of the larger area imaged for the stretched film. In both cases represented in figure 3 a racemic mixture has been used in the fabrication process. Nevertheless the morphology is similar for the right-handed enantiomer.

We observe similar elongated structures in all our measurements on stretched samples, independently of the drawing ratio and of the chromophore mixture. Such result, also confirmed by different microscopic diagnostics, can be interpreted by considering the growth mechanism of the polyethylene chains. According to Peterlin [26], the orientation of the lamellae of the original spherulitic or lamellar polymeric structure by mechanical drawing leads to rearranged material structures formed by microfibrils through a discontinuous process taking place at the micronecks located at the cracks of lamellae. Actually, during micronecking, the folded macromolecular chains are broken off, turned towards the drawing direction and produce the microfibrils consisting in alternate crystalline and amorphous regions.

Also maps of the optical quantities show rather different features in the as-cast and stretched films. Once more, the mechanical drawing process leads to the appearance of elongated domains in both γ and θ maps (figures 3(e) and (f), respectively), which correspond to regions with rather homogeneous linear dichroism values. By contrast, in the as-cast samples strong variations of optical quantities are

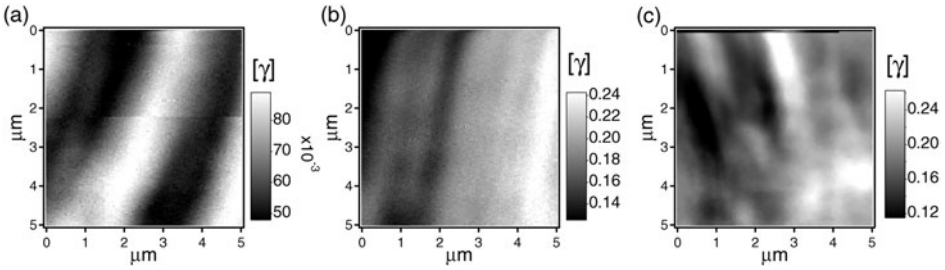

Figure 4. γ maps of films containing a 50:50 chromophore mixture at different drawing ratios (20×, 30× and 40×, (a), (b), (c), respectively).

observed, and randomly shaped domains appear. The value of the angle θ spans over all the permitted 90° range, and the dynamics of the γ map is rather large. Both findings suggest a random distribution and alignment of the dye molecules. Formation of spherulite-like structures is known to induce some degree of alignment in the guest molecules, but since no additional process is used to control the host chaining, the result is that the morphology of the observed domains is not organized along any preferential direction as it is in drawn films. On the other hand, formation of elongated optically active domains in stretched films confirms the effect of mechanical drawing on the mutual organization of the molecules, possibly induced by a quasi-epitaxial growth of the terthiophene molecules over the oriented polymer chain [27], enhanced by sample heating during the drawing process. This epitaxial-like process requires the presence of an aligning matrix during the domain formation. The efficiency of the process is obviously strongly enhanced when the chromophore molecules are present in the mixture while drawing is accomplished at suitable temperature. Nevertheless macroscopic analyses demonstrate a negligible polarizing efficiency for samples produced utilizing polymer film stretched prior deposition of molecules, suggesting that chromophore alignment is thereby not attained.

A comparison between panels (d)–(f) of figure 3 reveals that the morphology of the optically active domains does not completely reproduce the physical morphology of the surface. Topography and γ-maps are not fully correlated as expected if the space distribution and alignment of the dye molecules followed the crystallization of the polymer chain. Further analysis should address this point, whose interpretation requires a detailed understanding of the complex processes ruling molecular organization in host–guest systems. As a general trend, however, we note that stripes observed in optical maps, characterized by homogeneous values of γ and θ, exhibit a lateral size smaller (typically, a few hundreds of nanometres) than that of the topographical features (typically sized in the micrometre range). We cannot completely rule out that topographical variation is playing a role in our optical results. However, we have not found any systematic correlation between topography and optical maps, leading to the conclusion that our results are not due to optical features. In particular, enhancement of dichroism at topography borders would be expected in that case, and it is not generally observed.

The shape of the optically active domains in stretched films turn out to strongly depend on the fabrication parameters, in particular on the drawing ratio. As an example, figure 4 reports the γ maps for three samples containing the racemic mixture, and produced with different drawing ratios (20×, 30×, 40×). The lateral size of the elongated domains gets smaller for increasing drawing ratios. At the same time, the average value of γ increases at least up to the drawing ratio of 30× (the 40× case will be discussed briefly). Such an increasing trend of the linear dichroism as a function of drawing can be attributed to the increasing efficiency in aligning the dye molecules. This hypothesis is confirmed by the results of conventional polarimetry on our samples. Indeed, the $\overline{\gamma}$ value obtained by spatial averaging our maps is in agreement (but systematically slightly larger) with the dichroic ratio at the 488 nm wavelength measured by macroscopic methods. Our analysis demonstrates that the well known macroscopic behaviour of the films is due to the occurrence of sub-micrometre regions with homogenous anisotropic absorption.

The mesoscopic morphology of the samples is affected by the mechanical drawing with not completely expected features, at least when ultra-high molecular weight matrices are considered. We observe, as in figure 4(c), that larger drawing ratios lead to the formation of discontinuities and local inhomogeneities in the elongated optically active domains. Such circumstances are seldom reflected in the topographical maps, suggesting that the mechanisms governing distribution and alignment of the guest chromophore lose efficiency, even if the host matrix conserves a rather homogeneous morphology.

In a similar scenario, features of guest crystallization are expected to play an important role. According to macroscopic investigations based, e.g., on differential scanning calorimetry (DSC), it is known that chromophore crystallization depends on the kind of enantiomer mixture [28]. This effect is essentially associated with the different crystallization properties of the left- and right-handed enantiomers, leading to slightly different features in the phase segregation processes. The comparison between films produced with different chromophore mixtures, an example of which is shown in figure 5, reveals that the domain morphology is affected by the kind of enantiomer. The mesoscopic degree of organization, at 20× drawing ratio, is enhanced when the racemic mixture is employed, as demonstrated by the absence of fractures in figure 5(a). The film containing the right-handed enantiomer exhibits larger γ values, but at the expenses of space homogeneity, since fractures on the elongated domains are clearly seen. However, a complete interpretation of this result, which requires a careful analysis of crystallization features in the investigated samples, is out of the scope of the present work.

In order to support and complement our PM-SNOM analysis, we have carried out PL measurements under near-

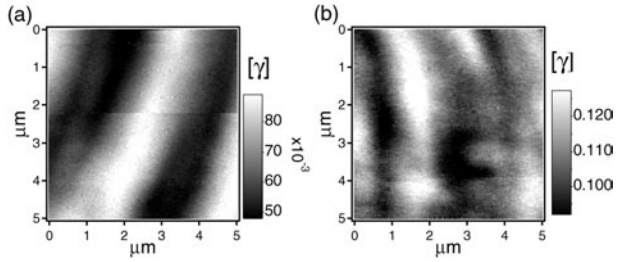

Figure 5. γ maps of films produced with a drawing ratio of 20× and containing a 50:50 enantiomer mixture (a) and right-handed enantiomer (b).

field excitation at 417 nm. In this case, a fixed polarization state for the exciting radiation is chosen and measurements with different choices of the polarization direction are repeated. We obtain a strong PL peaked around 500–530 nm. PL maps, not shown, are acquired in the reflection mode and compared with SNOM maps, simultaneously acquired in transmission. As expected, maximum emission stems from domains with maximum light absorption. This kind of analysis provides information on the chromophore space distribution complementary with respect to those acquired with PM-SNOM. More specifically, we infer a rather homogeneous space distribution of the dye molecules within the elongated domains typical of stretched films.

5. Conclusions

Linear dichroism of polymer-based films consisting of a mixture of chromophore molecules dispersed in a ultra-high molecular weight polyethylene matrix has been investigated on the local scale by using near-field microscopy. These results demonstrate that the PM-SNOM technique is able to unravel details of the optically active domains at the mesoscopic scale on this kind of samples. In particular, mechanical drawing turns out an efficient route to also induce molecule alignment on the mesoscale, in agreement with the findings of macroscopic polarimetry. On the other hand, the sub-micrometre space resolution offered by SNOM reveals features which cannot be observed with conventional approaches, such as inhomogeneities in the optical active domains occurring at large drawing ratios. Furthermore, differences in sub-micrometre scale domain morphology are found depending on the chromophore type (racemic mixture or right-handed enantiomer). Therefore our findings, besides providing us with recipes useful in the search for the optimal fabrication parameters, stimulate further work aimed at understanding the growth mechanisms taking place in host–guest systems.

References

[1] Pohl D W, Denk W and Lanz M 1984 *Appl. Phys. Lett.* **44** 651
[2] Novotny L, Pohl D W and Regli P 1994 *J. Opt. Soc. Am.* A **11** 1768
[3] Betzig E, Trautman J K, Harris T D and Wolfe R 1992 *Appl. Opt.* **81** 4563
[4] Tirelli N, Amabile S, Cellai C, Pucci A, Regoli L, Ruggeri G and Ciardelli F 2001 *Macromolecules* **34** 2129
[5] Gupta V K and Kornfield J A 1994 *Rev. Sci. Instrum.* **65** 2823
[6] Pucci A, Moretto L, Ruggeri G and Ciardelli F 2002 *e-Polymers* 015 http://www.e-polymers.org
[7] Pucci A, Ruggeri G, Moretto L and Bronco S 2002 *Polym. Adv. Technol.* **13** 737
[8] Eglin M, Montali A, Palmans A R A, Tervoort T, Smith P and Weder C 1999 *J. Mater. Chem.* **9** 2221
[9] Shindo Y and Ohmi Y 1985 *Rev. Sci. Instrum.* **56** 2237
[10] Lacoste Th, Huser Th, Prioli R and Heinzelmann H 1998 *Ultramicroscopy* **71** 333
[11] Vaez-Iravani M and Toledo Crow R 1993 *Appl. Phys. Lett.* **63** 138
[12] Goldner L S, Fasolka M J, Nougier S, Nguyen H P, Bryant G W, Hwang J, Weston K D, Beers K L, Urbas A and Thomas E L 2003 *Appl. Opt.* **42** 3864
[13] McDaniel E B, McClain S C and Hsu J W P 1998 *Appl. Opt.* **37** 84
[14] Wei P K and Fann W S 2001 *J. Microsc.* **202** 148
[15] Ramoino L, Labardi M, Maghelli N, Pardi L, Allegrini M and Patanè S 2002 *Rev. Sci. Instrum.* **73** 2051
[16] Wei P K, Lin Y F, Fann W, Lee Y Z and An Chen S 2001 *Phys. Rev.* B **63** 045417
[17] Fasolka M J, Goldner L S, Hwang J, Urbas A M, DeRege P, Swager T and Thomas E L 2003 *Phys. Rev. Lett.* **90** 016107
[18] Langeveld-Voss B M W, Beljonne D, Shuai Z, Janssen R A J, Meskers S C J, Meijer E W and Bredas J L 1998 *Adv. Mater.* **10** 1343
[19] Pucci A, Nannizzi S, Ruggeri G and Ciardelli F 2003 *16th Mtg on Macromolecules Science and Technology* (Pisa: Pacini Editore) p 361 (Book of abstracts)
[20] Ade H, Toledo Crow R, Vaez-Iravani M and Spontak R J 1996 *Langmuir* **12** 231
[21] Mark H F, Bikales N, Overberger C G, Menges G and Kroschiwitz J I 1985 *Encyclopedia of Polymer Science and Engineering* 2nd edn (New York: Wiley)
[22] Higgins D A, Vanden Bout D A, Kerimo J and Barbara P F 1996 *J. Chem. Phys.* **100** 13794
[23] Jalocha A and Van Hulst N F 1995 *J. Opt. Soc. Am.* B **12** 1577
[24] Karrai K and Grober R D 1995 *Appl. Phys. Lett.* **66** 1842
[25] Williamson R L and Miles M J 1995 *J. Vac. Sci. Technol.* B **4** 2
[26] Peterlin A 1977 *Polym. Eng. Sci.* **17** 183
[27] Jagt H, Dirix Y, Hikmet R and Bastiaansen C 1998 *Adv. Mater.* **10** 934
[28] Dumas J P 1978 *Appl. Phys.* **11** 1